



# Optimal Processing Scheme for meeting Cat II/III with the MC/MF GBAS

Alizé Guilbert, Carl Milner, Christophe Macabiau

► **To cite this version:**

Alizé Guilbert, Carl Milner, Christophe Macabiau. Optimal Processing Scheme for meeting Cat II/III with the MC/MF GBAS. NAVITEC 2014, 7th ESA Workshop on Satellite Navigation Technologies, Dec 2014, Noordwijk, Netherlands. <hal-01147313>

**HAL Id: hal-01147313**

**<https://hal-enac.archives-ouvertes.fr/hal-01147313>**

Submitted on 30 Apr 2015

**HAL** is a multi-disciplinary open access archive for the deposit and dissemination of scientific research documents, whether they are published or not. The documents may come from teaching and research institutions in France or abroad, or from public or private research centers.

L'archive ouverte pluridisciplinaire **HAL**, est destinée au dépôt et à la diffusion de documents scientifiques de niveau recherche, publiés ou non, émanant des établissements d'enseignement et de recherche français ou étrangers, des laboratoires publics ou privés.

# Optimal Processing Scheme for meeting Cat II/III with the MC/MF GBAS

NAVITEC 2014 3-5 December 2014  
ESA/ESTEC, Noordwijk, The Netherlands

Alizé Guilbert, Dr. Carl Milner, Dr. Christophe Macabiau  
TELECOM/SIGNAV Laboratory – ENAC, Toulouse, France  
7 Avenue Edouard Belin,  
31055 Toulouse Cedex 4, France  
Email: [guilbert@recherche.enac.fr](mailto:guilbert@recherche.enac.fr)

## ABSTRACT

To meet the long term goal of greater capacity in aviation, services must be expanded to provide more reliable and robust approach and landing operations in all weather conditions, globally using modernised navigation systems. This paper details the measurement processing techniques under investigation for the Multi-Constellation (MC) and Multi-Frequency (MF) Ground Based Augmentation System (GBAS) within the SESAR Framework Work Package 15.3.7. It deals with the performance improvements obtainable for CAT II/III precision approaches, the most stringent operation currently defined. GBAS has the potential to provide CAT II/III services without the need for expensive and regular maintenance and flight testing that comes with the current Instrument Landing System (ILS). Furthermore, in the case of ILS, multipath problems may restrict separation criteria in some conditions thus limiting capacity. SESAR WP15.3.7 is investigating a potential change in the message correction update rate. With the current correction rate of 2Hz it will not be possible to send multiple constellations and correction types beyond the bare minimum. This paper presents analyses relating to the error budget degradation when using lower frequency corrections.

## INTRODUCTION

To meet the long term goal of greater capacity whilst preserving safety in aviation, services must be expanded including reliable robust approach and landing operations in all weather conditions. GBAS Approach Service Type D (GAST D), designed to meet CAT II/III performance requirements using a single frequency (L1 C/A) of the Global Positioning System is at an advanced stage of development and standardisation but open questions remain and availability will not be assured for installations worldwide, all of the time. Adding the Galileo constellation will provide improved geometry and offer a redundant civilian owned system. Therefore, European research is addressing the transition from single frequency GBAS to Dual-Constellation (DC), Dual-Frequency (DF) GBAS. Galileo and modernized GPS will provide signals on two protected frequency bands such that DF processing can improve performance through mitigation of ionospheric errors (gradients, plasma bubbles, scintillations). GAST-D faces demanding constraints (siting, threat model and monitoring concept validation) linked to requirements protecting against anomalous ionospheric conditions.

DC/DF GBAS has the potential to relax these constraints thus improving availability, coverage and access to CAT II/III operation. Furthermore, safety can be expected to be improved since all theoretical ionospheric events are likely to be protected against and any unscheduled operational outages as a result will be likely reduced significantly over the GAST D solution. This paper first presents GBAS processing architecture. Error models are then presented which critically contribute to the range-rate corrections. The properties of the range-rate corrections are key to understanding how an increase in the correction update period will impact the total performance of the system. The total error budget is then derived which allows a quantification of the degradation in the corrections as a function of the message update rate. Theoretical curves are then presented for the current MT1 and MT11 corrections based on 100s and 30s smoothing constants respectively. Furthermore, a real data analysis performed with single frequency GPS L1 data to validate models and to compare results with the theoretical curves obtained is presented. Indeed, several simulations for analysing the influence of an increased update rate of PRC and RRC were processed by comparing extrapolation of PRC for 1.5s with extrapolation of PRC for other extended times. Finally, conclusions about error model modifications and the feasibility of an extension of a correction update period to a few seconds are given.

## GAST D PROCESSING ARCHITECTURE

The GBAS ground subsystem processing (described in Fig. 1) must transmit through the VHF Data Broadcast (VDB) unit several message types which include the correction parameters for each satellite (according to MOPS [1]): Pseudo Range Correction (PRC) and Range Rate Correction (RRC).

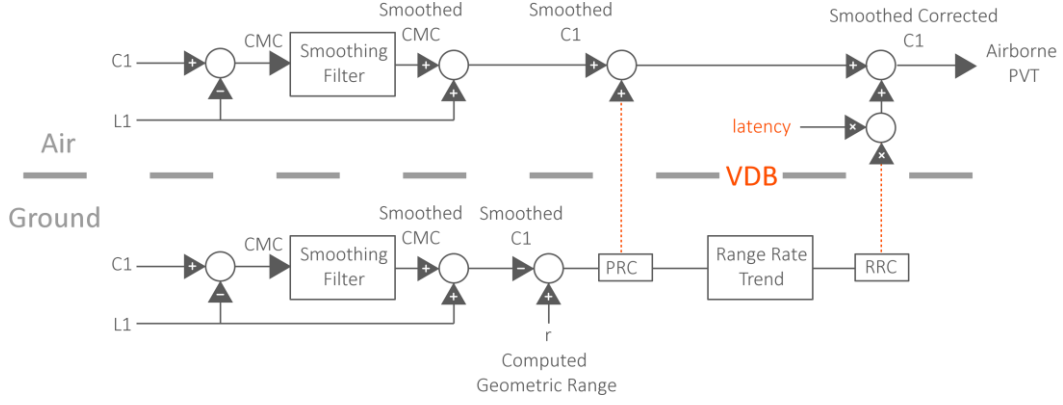


Fig. 1 – GBAS Processing Architecture

For GAST D both Message Type 1 (MT1) and Message Type 11 (MT11) are used to provide corrections with both 100s and 30s smoothing respectively [2] [1] [3]. The longer smoothing constant corrections in MT1 mitigate to a greater extent the high frequency components of multipath and noise but suffer from greater ionospheric divergence than the 30s corrections contained in MT11. The measurement model used in this paper is as follows [4] [5]:

$$\rho_1^G = r^G + dr^G + b^G + J^G - \iota_1^G + \eta_{\rho_1}^G \quad (1)$$

$$\phi_1^G = r^G + dr^G + b^G + J^G - \iota_1^G + N_1^G + \eta_{\phi_1}^G \quad (2)$$

Where  $r$  is the true range,  $\rho$  is the pseudorange measurement,  $\iota$  is the ionospheric delay,  $J$  is the tropospheric delay,  $dr$  is the ephemeris error,  $b$  is the satellite clock error,  $\eta_{\rho}$  is the code-tracking noise and multipath,  $\phi$  is the carrier-phase measurement,  $N$  is the range ambiguity and  $\eta_{\phi}$  is the carrier-tracking noise and multipath.  $\blacksquare_1$  represents a variable for on the L1 signal,  $\blacksquare^G$  is used for parameters relating to the ground receivers and  $\blacksquare^A$  for those relating to the airborne receiver. Recalling the correction definitions and their associated models [1]:

$$PRC_1 = r^G - \hat{\rho}_1^G = -dr^G - b^G - J^G - \iota_1^G - \epsilon_1^G \quad (4)$$

$$RRC_{1,k} = \frac{PRC_{1,k} - PRC_{1,k-1}}{T} = -d\dot{r}^G - \dot{b}^G - \dot{J}^G - \dot{\iota}_1^G - \dot{\epsilon}_1^G \quad (5)$$

Where  $\hat{\rho}_1^G$  is the smoothed pseudorange observable,  $I$  is the smoothed ionospheric delay,  $\epsilon$  represents smoothed multipath and noise components and  $\blacksquare$  defines the linear derivative. The influence of the PRC-based receiver clock correction has been neglected in equations (4) and (5) as it introduces common mode-like errors which cancel in the airborne position solution. At the airborne receiver, the corrections are applied using the following expression:

$$\tilde{\rho}_1^A(t_A) = \hat{\rho}_1^A(t_A) + PRC_1 + t_{AZ}RRC_1 \quad (6)$$

Where  $t_{AZ}$  represents the time between the modified time of correction generation  $t_z$  and the time of application at the airborne receiver:  $t_{AZ} = t_A - t_z$ .  $\hat{\rho}$  is the smoothed pseudorange measurement and  $\tilde{\rho}$  is the corrected pseudorange measurement. Equation (6) may be decomposed using equations (4) and (5) into the error components.

$$\begin{aligned} \tilde{\rho}_1^A(t_A) = r^A + (dr^A - (dr^G + t_{AZ}d\dot{r}^G)) + (b^A - (b^G + t_{AZ}\dot{b}^G)) + (J^A - (J^G + t_{AZ}\dot{J}^G)) \\ + (I_1^A - (I_1^G + t_{AZ}\dot{I}_1^G)) + (\epsilon_1^A - (\epsilon_1^G + t_{AZ}\dot{\epsilon}_1^G)) \end{aligned} \quad (7)$$

## SINGLE FREQUENCY ERROR MODELS

### Ground Multipath and Noise

The residual error at the airborne receiver due to smoothed code multipath and noise can be described with the following equation:

$$\delta\epsilon = \epsilon_1^A - (\epsilon_1^G + t_{AZ}\dot{\epsilon}^G) \quad (8)$$

It is important to note that the term  $\dot{\epsilon}^G$  is the error contribution due to the change in the smoothed ground multipath and noise over the interval  $T$  at epoch  $k$ .

$$\dot{\epsilon}^G = \frac{\epsilon_{1,k}^G - \epsilon_{1,k-1}^G}{T} \quad (9)$$

Under the assumption of uncorrelated raw multipath and noise terms the residual error follows a zero-mean Gaussian distribution defined by:

$$\delta\epsilon \sim N(0, \sigma_\epsilon^2) \quad (10)$$

$$\sigma_\epsilon^2 = \sigma_{\epsilon^A}^2 + \sigma_{\epsilon^G}^2 + (t_{AZ})^2 \sigma_{\dot{\epsilon}^G}^2 \quad (11)$$

and  $\sigma_{\epsilon^A}$  is the standard deviation of the airborne multipath and noise,  $\sigma_{\epsilon^G}$ , the standard deviation of the multipath and noise on the pseudorange correction and  $\sigma_{\dot{\epsilon}^G}$  the standard deviation of the multipath and noise contribution to the RRC. The difference over two epochs in smoothed multipath and noise at the ground is then [6]:

$$\epsilon_{1,k}^G - \epsilon_{1,k-1}^G \approx \eta_{1,\rho,k}^G \frac{T}{\tau} + \sqrt{2}\eta_{1,\phi,k}^G \quad (12)$$

where  $\eta_{1,\rho,k}^G$  is defined as the raw code multipath and noise component,  $\eta_{1,\phi,k}^G$  is defined as the phase multipath and noise component and  $\tau$  as the smoothing time constant, giving:

$$\dot{\epsilon}^G \approx \frac{\eta_{1,\rho,k}^G}{\tau} + \frac{\sqrt{2}}{T}\eta_{1,\phi,k}^G \quad (13)$$

The standard deviation of the contribution to the error rate in the smoothed multipath and noise can be expressed as:

$$\sigma_{\dot{\epsilon}^G} \approx \sqrt{\left(\frac{\sigma_{\eta_{1,\rho}^G}}{\tau}\right)^2 + 2\left(\frac{\sigma_{\eta_{1,\phi}^G}}{T}\right)^2} \quad (14)$$

A conservative bound of 3mm is assumed for the phase noise element of  $\sigma_{\eta_{1,\phi}^G}$  (the impact of phase multipath is under review). Values of  $\sigma_{\eta_{1,\rho}^G}$  as a function of elevation have been obtained from the DLR experimental GBAS installation which is described in [7]. This elevation dependent model is likely conservative with respect to an operational station.

### Ionosphere + Troposphere

The single frequency differential residual error due to the ionospheric and tropospheric delays are expressed as follows:

$$\delta I = I_1^A - (I_1^G + t_{AZ}I_1^G) \quad (15)$$

$$\delta J = J^A - (J^G + t_{AZ}J^G) \quad (16)$$

In order to address the 2<sup>nd</sup>-order temporal effects of the nominal ionosphere and troposphere errors, they may be decomposed into spatial and temporal components.

$$\delta I = \underbrace{I_1^A(t_A) - I_1^G(t_A)}_{\text{spatial}} + \underbrace{I_1^G(t_A) - (I_1^G(t_G) + t_{AZ}I_1^G)}_{\text{temporal}} \quad (17)$$

$$\delta J = \underbrace{J^A(t_A) - J^G(t_A)}_{\text{spatial}} + \underbrace{J^G(t_A) - (J^G(t_G) + t_{AZ}j^G)}_{\text{temporal}} \quad (18)$$

Note that in nominal conditions when the smoothing filters within the ground and airborne subsystems are in steady states, the term  $J_1^G$  can be considered as a constant such that the temporal component will be zero and the residual differential ionospheric error will contain only a spatial component. It is currently under investigation within SESAR WP 15.3.7 as to whether  $J^G$  can be considered as a constant over the period of three smoothing windows. If so the residual differential error due to the troposphere will contain only a spatial component.

### Satellite Clock Error

The residual differential error due to Satellite Clock can be modelled with a zero-mean Gaussian [5]:

$$\delta b = b^A - (b^G + t_{AZ}\dot{b}^G) \quad (19)$$

$$\delta b \sim N(0, \sigma_b^2) \quad (20)$$

where  $\sigma_b$  is defined as it is described in details in [5] by the following expression:

$$\sigma_b^2 = \left(1 + \frac{t_{AZ}}{T}\right) t_{AZ} AVAR(1s) \quad (21)$$

with  $AVAR(1s)$  representing the Allan Variance at the order of 1s.

As it is explained in [5], the residual stochastic satellite clock time error after applying the PRC is a random walk resulting from the sum of independent Gaussian random variables. Since GBAS provides scalar corrections in the form of the PRC and RRC all the error types are combined. The RRC contains a term that corresponds to the satellite clock error rate, which in the mean will correspond to the deterministic component of the error that was not perfectly estimated by the constellation control segment and modelled by the broadcast clock correction clock error rate term. In [5], the effect of this linear prediction is analysed. The conclusion is that it increases the residual satellite clock error by a factor  $\sqrt{\left(1 + \frac{t_{AZ}}{T}\right)}$  with respect to the error without applying the linear prediction correction.

By incorporating the impact of the RRC we obtained the Fig. 2 representing the residual satellite clock error as a function of  $t_{AZ}$  for the case where  $T = 0.5s$ . The standard deviation rises to a few centimetres for the worst performing GPS satellite over update periods up to 10s. Also, we note that with the improved expected performance for the Galileo clock over this time scale only a very small growth in the residual error standard deviation is seen. With regard to the clock errors, an extension of an update period (increasing of  $t_{AZ}$ ) to a few seconds appears feasible.

### Residual Ephemeris Error

The residual differential error due to Residual Ephemeris can be modelled by:

$$\delta dr = dr^A - (dr^G + t_{AZ}d\dot{r}^G) \quad (22)$$

As was the case for the environmental errors, we may split the error into spatial and temporal components:

$$\delta dr = \underbrace{dr_1^A(t_A) - dr_1^G(t_A)}_{\text{spatial}} + \underbrace{dr_1^G(t_A) - (dr_1^G(t_G) + t_{AZ}d\dot{r}^G)}_{\text{temporal}} \quad (23)$$

The RRC corrects for  $d\dot{r}^G$ , the temporal component is negligible and the mm level spatial error remains.

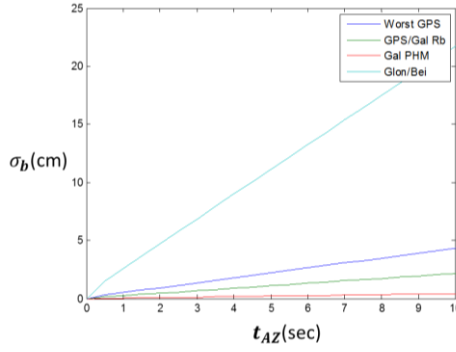


Fig. 2 – Standard deviation of the Residual Satellite Clock Error over time

### Total Error

The RRC may be modelled at each epoch as containing a bias term relating to the true linear variation from ephemeris, satellite clock ionosphere and troposphere error rates as well as a stochastic term as a result of the code and phase multipath and noise, the stochastic satellite clock error and other random errors. The VDB data (e.g. Fig. 8) shows that the RRC bias is negligible with respect to its noise. The total error model for  $\tilde{\rho}_1^A(t_A)$  can be expressed as follows:

$$\tilde{\rho}_1^A(t_A) \sim N(0, \sigma^2) \quad (24)$$

with

$$\sigma^2(\tau, \Delta t_G, t_{AZ}, el) = \underbrace{\left( \frac{(\sigma_\eta(el)T/(2\tau))^2}{SV\ clock} + \frac{(t_{AZ})^2 \left( \left( \frac{\sigma_{\eta_{1,\rho}}^G(el)/\tau}{air\ multipath\ +\ noise} \right)^2 + 2 \left( \frac{\sigma_{\eta_{1,\phi}}^G/T}{iono} \right)^2 \right)}{tropo} \right)}_{\text{iono}} + \frac{\sigma_{\epsilon^A}^2(el)}{tropo} \quad (25)$$

Note that variations in smoothing filter type and time constant will impact  $\sigma_{\epsilon^A}$ ,  $\sigma_\eta$  &  $\sigma_{iono}$ . The impact of the correction update period extension has been derived. The standard deviation of the total error model for the corrected smoothed airborne pseudorange  $\tilde{\rho}_1^A(t_A)$  was determined for different processing options using the existing single-frequency smoothed observable and on the ionosphere-free (IF) and differing the smoothing constants. In this paper, only GPS L1 C/A and GPS L1/L5 IF are presented, though little dependency on constellation clock performance was found. Therefore, these results may be used for equivalent Galileo observables

Fig. 3 shows the impact of elevation and  $t_{AZ}$  on the total standard deviation for GPS L1C/A and for the GPS L1-L5 IF case [4]. Empirical values from SESAR WP 15.3.7 are used for the ground code multipath component whilst an AAD B level is taken for the aircraft installation [1]. Fig. 4 shows the difference in the standard deviation of the corrections for different extrapolation times of the GPS L1 C/A. The 30s standard deviation is higher than the 100s but in both cases, the highest value is of the order of 20cm. There is only a minor difference of a couple of centimetres for update periods up to five seconds. Fig. 5 depicts the impact of elevation on RRC for both 30s and 100s smoothing constants.

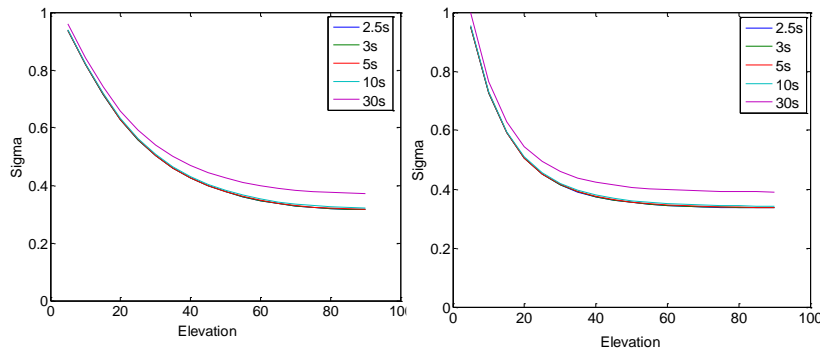


Fig. 3 - Impact of elevation and  $t_{AZ}$  on the total standard deviation for GPS L1C/A (left) and GPS L1-L5 IF (right)

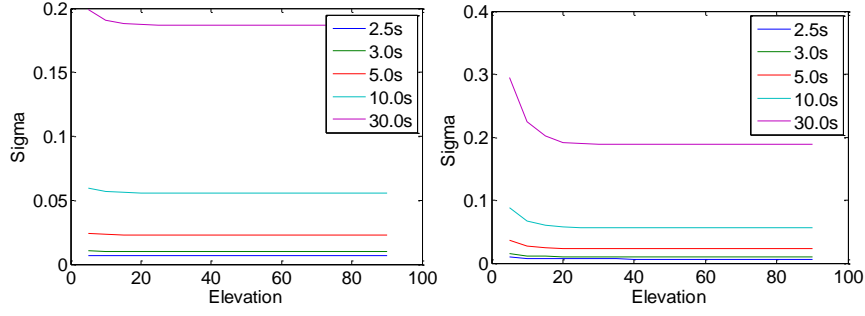


Fig. 4- 100s (left figure) and 30s (right figure) Smoothed Error Degradation with Update Period

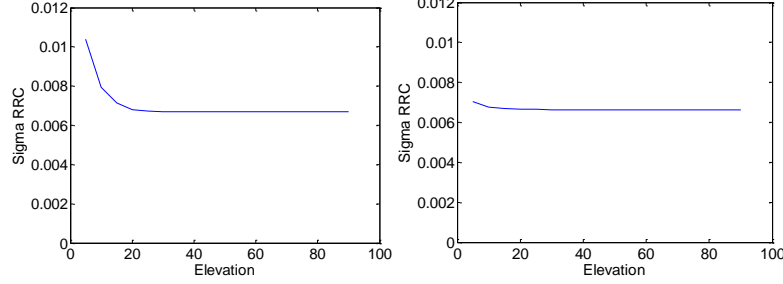


Fig. 5 – 100s (left figure) and 30s (right figure) smoothed RRC

## DATA PROCESSING METHODOLOGY

According to the current GAST D requirements [3] based on the 2Hz correction rate,  $t_{AZ}$  must be inferior to 1.5s in the absence of lost VDB messages and airborne related delays. If the update period of the PRC is extended, this value will increase. There is then the need to examine the influence of higher  $t_{AZ}$ . In order to analyse the influence of an increased correction update period the current extrapolation of PRC of 1.5s was compared to longer extrapolation times  $t_{ex}$ . Fig. 6 shows at the airborne receiver time  $t$  the difference between extrapolated PRC computed using PRC at  $t$ . The following computation expresses the difference in the error using a longer extrapolation period to the current approach:

$$PRC_{t_{ex}}(t) = PRC(t - t_{ex}) + RRC(t - t_{ex}) \times t_{ex} \quad (26)$$

$$PRC_{1.5}(t) = PRC(t - 1.5) + RRC(t - 1.5) \times 1.5 \quad (27)$$

$$\delta PRC_{1.5}(t) = |PRC_{1.5}(t) - PRC_{smooth}(t)| \quad (28)$$

$$\delta PRC_{t_{ex}}(t) = |PRC_{t_{ex}}(t) - PRC_{smooth}(t)| \quad (29)$$

$$\Delta PRC_{t_{ex}-1.5}(t) = \delta PRC_{t_{ex}}(t) - \delta PRC_{1.5}(t) \quad (30)$$

where  $PRC_{smooth}$  is the reference ‘true’ PRC obtained using a 20 point Gaussian filter. The set of positive  $\Delta PRC_{t_{ex}-1.5}$  is used to derive the statistics as this conservatively relates to the degradations in performance. The  $\Delta PRC$  will depend upon the statistical properties of the  $RRC$  which in turn may depend upon elevations. The standard deviations for the RRCs from MT1 and MT11 for  $5^\circ$  elevation bins are determined.

## DATA PROCESSING RESULTS

One day of VDB message data obtained from the Thales GAST D prototype ground station installed at Toulouse Blagnac airport was processed. Fig. 7 shows histograms of the RRC over all ranging sources for the MT1 and MT11 corrections. It is clear that these RRC distributions are central and in fact contain a high number of zero values (note that the resolution of the RRC is 1mm/s). Standard deviations for RRCs from MT1 and MT11 were plotted as a function of elevation in Fig. 8. Fig. 8 also shows a typical one minute interval of the RRC and its characteristic noise-like nature. The standard deviation of RRC for MT1 takes values from 3-7mm/s and for MT11 takes values from 5-8mm/s. These intervals are similar but smaller than those found in theory (Fig. 5) where we have values from 7-10mm/s. Finally, Fig. 9 presents the standard deviations of  $\Delta PRC$  for MT1 and MT11 for different update periods.

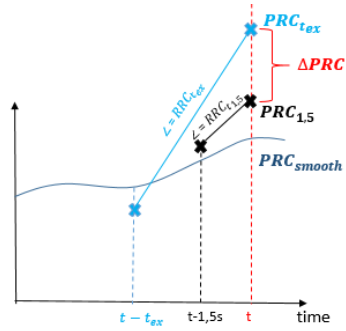


Fig. 6– PRC and RRC over time

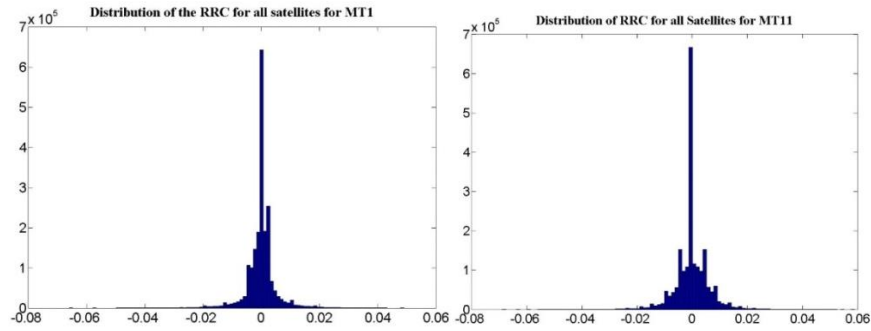


Fig. 7 – Distribution of RRC for all satellites for MT1 (left figure) and MT11 (right figure)

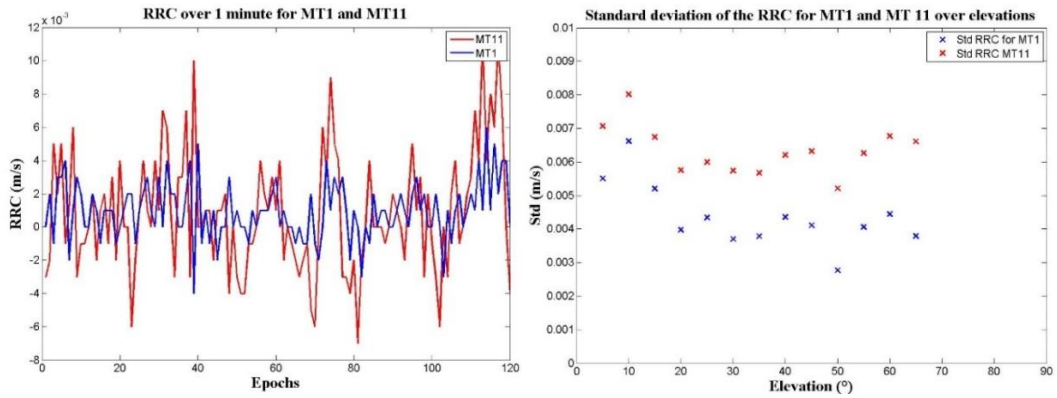


Fig. 8 – RRC over 1minute (left) and Standard deviation of RRC (right) for MT1 (blue) and MT11 (red)

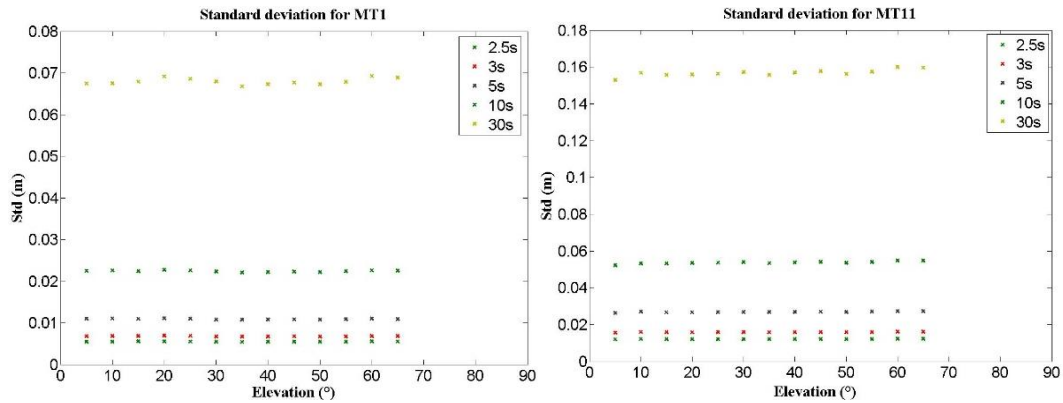


Fig. 9 – Standard deviation of  $\Delta PRC$  for different time of extrapolation



The Fig. 9 shows little dependency on elevation as was determined from the theoretical results and appears to confirm that the phase noise whose level only has a minor dependence on elevation is the primary contributor. However, the empirical results (Fig. 8 and Fig. 9) show a greater influence of the smoothing constant than as determined theoretically (Fig. 4). Indeed, the highest value for standard deviation is around 7cm for MT1 and 16cm for MT11 in the empirical curves and around 18 cm for MT1 and around 20cm for MT11. This analysis suggests that the contribution of code multipath and noise is not sufficiently modelled in the theoretical derivation.

## SUMMARY

This paper has addressed the question of whether decreasing the frequency of correction messages in GBAS severely degrades the performance of the differential correction process under nominal, fault-free conditions. An enhanced derivation of the differential satellite clock error has been presented and how the ground multipath and noise effects on both code and phase are inflated through the use of the RRC were analysed.

The total error budget was derived to quantify the degradation as a function of the message update rate for the current MT1 and MT11 corrections based on 100s and 30s smoothing constants respectively. Theoretically, the standard deviations rise by a couple of centimetres over update periods up to 10s and thus an extension of the update period from nowadays 0.5s to say 3.5s appears feasible. As seen in the derivation of the IF smoothing, this effect will be inflated when using IF. The real data analysis found similar results to those derived theoretically and as expected due to conservative nature of the theoretical assumptions, the standard deviations of the resulting errors were smaller. The impact of smoothing between the two approaches requires further work.

## ACKNOWLEDGEMENTS

The authors would like to thank the DSN and Thales Electronic Systems for the provision of data from the prototype GAST D ground station and partners of the SESAR WP 15.3.7. They would also like to thank Frieder Beck for his advice regarding the ground subsystem extrapolation computations.

*“©SESAR JOINT UNDERTAKING, 2013. Created by ENAC, DSN and Thales Electronic Systems for the SESAR Joint Undertaking within the frame of the SESAR Programme co-financed by the EU and EUROCONTROL. The opinions expressed herein reflect the author's view only. The SESAR Joint Undertaking is not liable for the use of any of the information included herein. Reprint with approval of publisher and with reference to source code only.”*

## REFERENCES

- [1] RTCA Inc., Minimum Operational Performance Standards (MOPS) for GPS Local Area Augmentation System (LAAS) Airborne Equipment - RTCA DO-253C, Washington DC, 2008.
- [2] RTCA Inc., MASPS for LAAS - RTCA DO-245A, Washington DC, 2004.
- [3] RTCA, Inc, RTCA DO-246D - GNSS-Based Precision Approach Local Area Augmentation System (LAAS) Signal-in-Space Interface Control Document (ICD), 2008.
- [4] P. Y. M. G. A. & B. J. R. HWANG, Enhanced Differential GPS Carrier-Smoothed Code Processing Using Dual-Frequency Measurements. Journal of The Institute of Navigation, Vol 46 numero 2., 1999.
- [5] SESAR(JU), «Satellite constellations and Signals - Int ST3.3-WP15.03.07 Multi GNSS CAT II/III GBAS,» 2014.
- [6] SESAR(JU), «INT. D3.6.1-ST3.6 Initial Processing Options, SW Requirements and Test Plan,» 2014.
- [7] M.-S. Circiu, M. Felux, P. Remi, L. Yi, B. Belabbas et S. Pullen, «Evaluation of Dual Frequency GBAS Performance using flight Data,» *ITM 2014*.
- [8] NSP working group, GBAS CAT II/III Development Baseline SARPs, 2010.
- [9] G. A. McGraw, «Generalized Divergence-Free Carrier Smoothing with Applications to Dual Frequency Differential GPS,» chez *ION NTM 2006*, Monterey, CA, 2006.